Infrared Telescope Technology Testbed primary mirror test results

Andrew E. Lowman, Steven A. Macenka, David C. Redding, Scott A. Basinger

Jet Propulsion Laboratory (JPL)
Pasadena, CA 91109

ABSTRACT

An 85 cm aperture beryllium mirror was fabricated as part of the Infrared Telescope Technology Testbed (ITTT), a facility to which the SIRTF flight telescope will be traceable. The ITTT was developed to demonstrate that diffraction-limited performance at a wavelength of 6.5μm is attainable from an ultra-lightweight meter-class beryllium telescope operating at a temperature of 5.5K. Cryo-null figuring was employed to meet the requirements for the shape of the primary mirror at its operating temperature over an aperture of 79cm. The results of this process will be presented, including the repeatability of the surface through cryogenic temperature cycling. Modeling of system performance using the residual figure error will be described. Image-based methods were used to characterize a turned up edge that is too steep to be measured with an interferometer.

Keywords: SIRTF, space optics, optical testing, optical fabrication, beryllium

1. INTRODUCTION

The Space InfraRed Telescope Facility (SIRTF), the infrared sibling of the Hubble Space Telescope, will be launched in late 2001.[1,2] Its cold telescope assembly will be an 85cm aperture Ritchey-Chretien telescope of all-beryllium construction with an operating temperature of 5.5K. Diffraction limited performance is required for wavelengths greater than 6.5μm. To demonstrate the critical technologies for this and other future projects, the Infrared Telescope Technology Testbed (ITTT) was developed.[3-5]

ITTT consists of an 85cm aperture ultra-lightweight beryllium telescope. The optics for ITTT were fabricated by Hughes Danbury Optical Systems (HDOS).[6] In parallel, the SIRTF Telescope Test Facility (STTF) was constructed at JPL for component and system level optical testing at low temperature. STTF is a large vacuum chamber, mounted on vibration isolators, with cooling by both liquid nitrogen and liquid helium. A platform below the chamber holds a phase-shifting interferometer (Zygo GPI). Separate null correctors were designed and fabricated by JPL and HDOS to test the ITTT primary mirror at its center of curvature. HDOS also developed an error budget to give the telescope diffraction limited performance at 6.5μm. The amount budgeted to the primary mirror surface error is 0.125μm, or 0.20λ rms at a wavelength of 633nm. To achieve this target at low temperature, cryo-null figuring was employed. Results of this process and other measurements of the mirror will be discussed, along with the expected performance.

2. CRYO-NULL FIGURING

The primary mirror has a single arch design with attachment by flexures in three places. The center of the mirror is a relatively thick 4cm, but this tapers to 6mm at the edge. As the primary is cooled to low temperature, the surface takes on a multi-lobed astigmatic shape. Extensive testing was conducted to ascertain that the source of this deformation was the mirror itself and not the mount or part of the test setup.[3] To compensate for this change, the mirror was polished using cryo-null figuring, a process whereby the figure is measured at low temperature and the inverse shape polished into the surface at room temperature, using small tools on a computer controlled polishing machine. This method has previously been applied successfully to fused quartz.[7]

Before attempting to correct the cryogenic distortion, repeated temperature cycling was performed to test for thermal hysteresis. The first ambient measurement taken in the STTF showed an rms surface error of 0.19λ, with a peak-to-valley

(PV) of 1.56λ (figure 1). The error was dominated by concentric zones, a result of the grinding process. (The rough figure was generated by rotating a form tool of the correct shape for the mirror, with no lateral stroke applied since the surface is aspheric.) After five cycles to 77K and three to 5K, over a period of several months, the ambient figure was essentially unchanged at 0.19λ rms, 1.35λ PV. The uncertainty in the JPL measurements is estimated to be <±0.02λ rms; PV numbers are less consistent due to their sensitivity to the odd misbehaving data point.

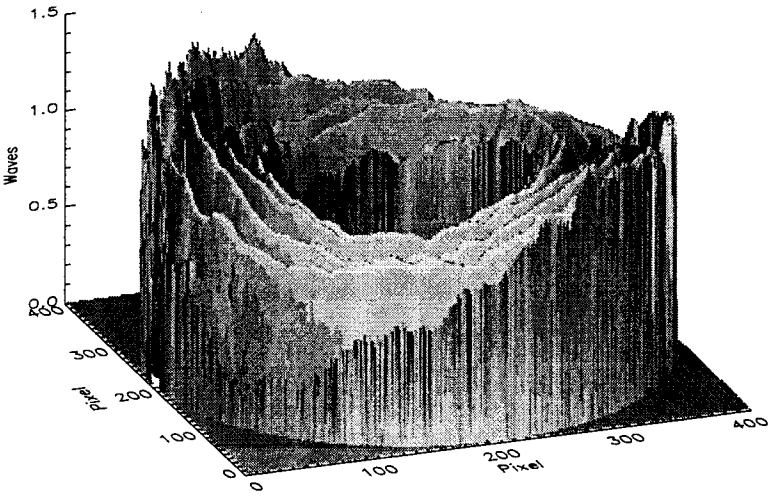

Figure 1. Surface figure error at ambient (rms = 0.19λ)

The surface figure at 5K has an rms error of 0.59λ, with a PV of 4.30λ (figure 2). At 77K the figure (0.58λ rms, 4.42λ PV) is essentially identical to the 5K figure, an expected result since the coefficient of thermal expansion for beryllium is very small (0.001ppm/K) in this temperature range.

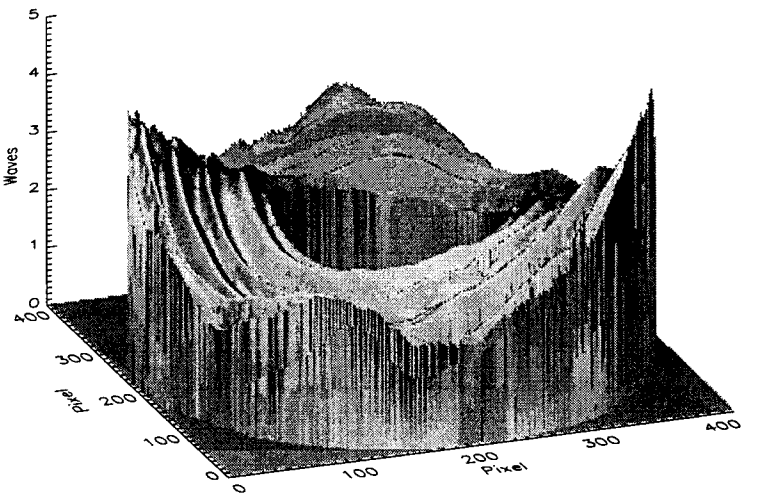

Figure 2. Surface figure error at 5K (rms = 0.59λ)

After the cryo-null figuring cycle, the ambient figure error increased to 0.44λ rms (3.45λ PV). At 77K, this dropped to 0.15λ rms (1.38λ PV). The data were consistent through three temperature cycles between ambient and 77K. Due to a leak in the helium tank, the mirror could only be cooled to about 20K; at this temperature, the figure was essentially identical to the 77K measurement. A 24K measurement is shown in figure 3.

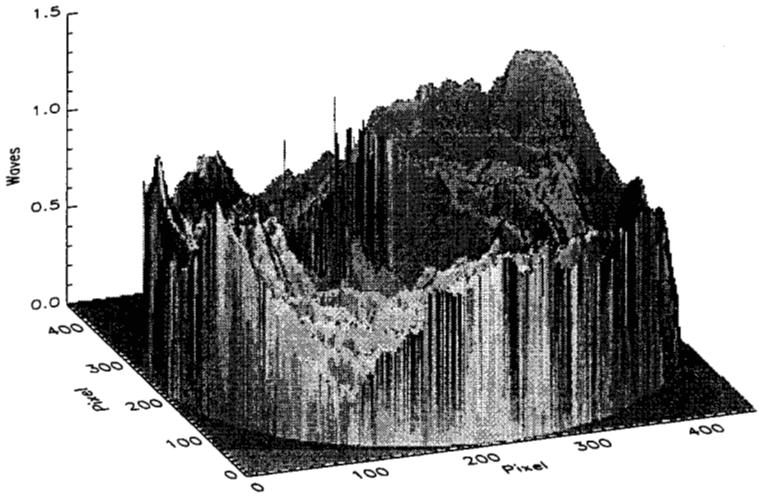

Figure 3. Surface figure error at 24K after cryo-null figuring (rms = 0.15λ)

The 24K measurement of 0.15λ rms is within the error budget of 0.20λ for the primary mirror. This represents a factor of four improvement in the low temperature surface figure. Unfortunately, these measurements only cover approximately 79cm of the desired 85cm clear aperture. The mirror has an upturned edge, with a slope too steep to be measured interferometrically. This will be discussed later in the paper.

3. EXPECTED PERFORMANCE

The residual surface error at low temperature contains strong mid-spatial frequency errors (predominantly concentric rings). Their magnitude is greatly reduced from the initial figure, but still noticeable in a surface map. These will have a minimal impact at 6.5μm; however, they will have a strong impact at shorter wavelengths. This was modeled in CodeV®.[8]

A model was created by incorporating the low temperature figure measurement into prescriptions of the SIRTF telescope. The JPL null corrector produces approximately 10% pupil distortion, so this had to be removed. A prescription for the null test was set up in CodeV®, with the measured wavefront placed at the entrance pupil of the system. A rectangular grid of rays was traced to the mirror surface, with the resulting optical path difference (OPD) at each point on the surface written to a file. This yielded an undistorted primary mirror map. A few points near previously missing data produced errant results due to interpolation across the gaps, so these were removed.

In order to use the entire 85cm aperture, some image processing was performed to fill in missing data points, including simulation of what the steep edge would look like if corrected. Zernike polynomials were fit to the now undistorted map, to separate low order aberrations from the mid-spatial frequency errors. The fitting was restricted to 15 Zernike terms (FRINGE-style, up through fifth order spherical aberration), to avoid steep edges that might result with higher order terms when extrapolating the aperture from 79cm to 85cm. At missing data points, the Zernikes were simply extrapolated using the appropriate coordinates. A polynomial of the form cosine(10ρ) and magnitude similar to the higher order errors was used to simulate the mid-spatial frequency errors in these regions. A boxcar filter was applied at the boundary between

valid and missing data points, to eliminate sharp transitions at the interface. The resulting map was applied to the primary mirror in CodeV®.

The secondary mirror figure data was also incorporated into the model.[9] Only ambient data is available for this optic; building and certifying a Hindle sphere at cryogenic temperatures would be a very expensive proposition, and any cryogenic distortion of this mirror could in theory be extracted in a much more cost-effective manner from a test of the assembled telescope. The secondary mirror was then tilted and decentered to simulate alignment errors, with their magnitude set to give the telescope diffraction limited performance ($\lambda/14$ rms) at the edge of the field at 6.5μm.

Point spread functions on-axis at three wavelengths (6.5μm, 3.5μm, and 0.6μm) are shown in figure 4, with the corresponding encircled energies plotted in figure 5. At 6.5μm, performance is diffraction limited, and the mid-spatial frequency content only shifts a small amount of energy beyond the 80% point to the outer rings of the Airy disc. However, performance will be worse for shorter wavelength instruments, and the mid-spatial frequency errors will strongly influence the shape of the PSF used at visible wavelengths for the SIRTF pointing calibration and reference sensor (PCRS).[10]

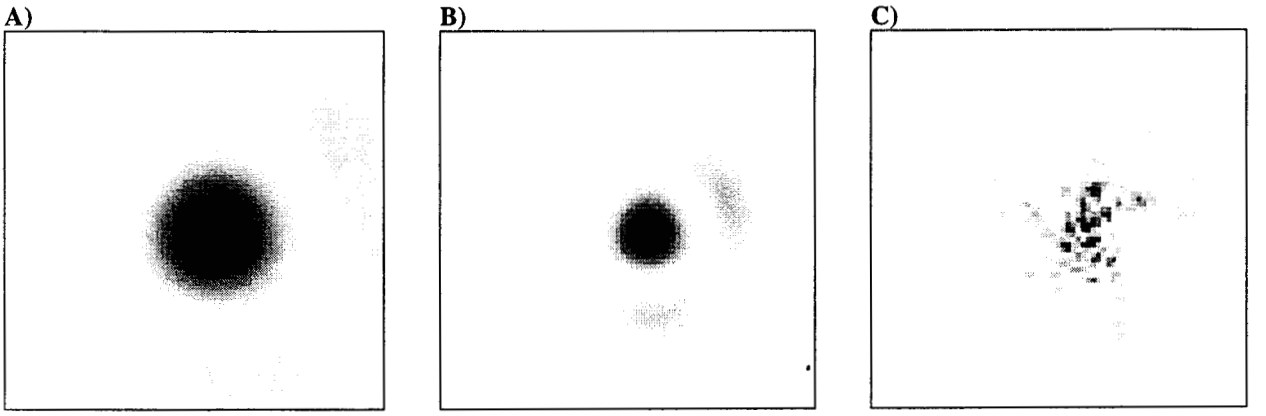

Figure 4. Point spread functions for (A) 6.5μm, (B) 3.5μm, and (C) 0.6μm. Each image is 300μm X 300μm.

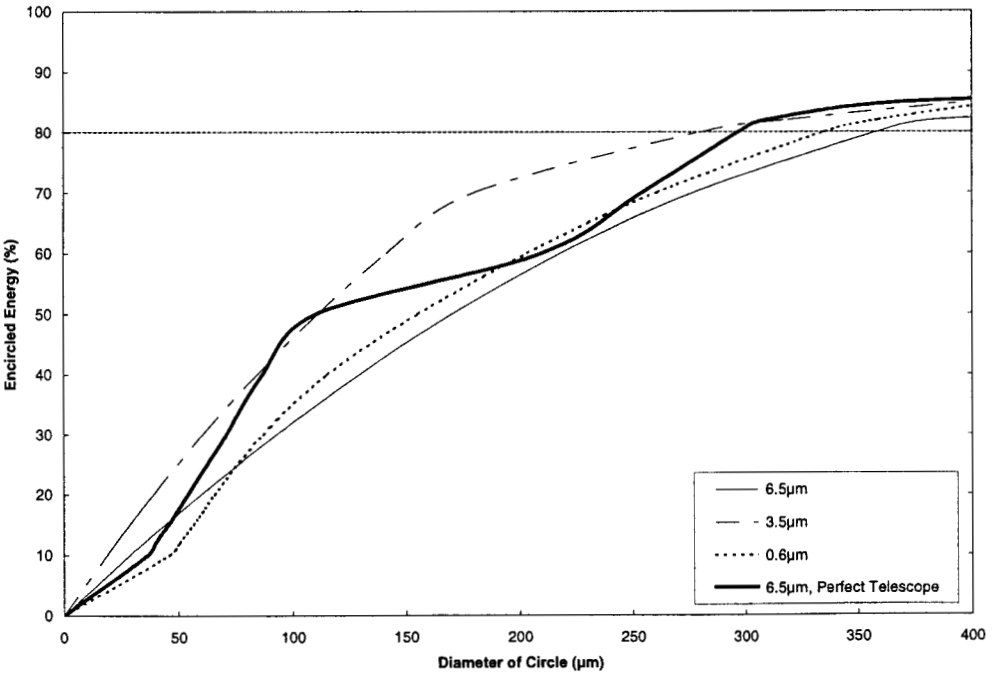

Figure 5. Encircled energy plots.

4. EDGE MEASUREMENT

The beryllium primary was stress relieved at various stages of fabrication. During the thermal cycling following 5μm grinding, the edge of the mirror changed shape, resulting in a turned up edge. To avoid slippage in the schedule for demonstrating cryo-null figuring, a decision was made to proceed with polishing and fix the edge later, if desired, rather than regrinding at that point.

The edge was improved during initial polishing; however, during the cryo-null figuring process, the slope became steeper. Part of the wavefront from this portion of the wavefront is too steep for its fringes to be resolved by the camera in the interferometer. Most of this portion of the wavefront never makes it to the camera, due to vignetting in the optics and cryo chamber.

Profilometry data taken at HDOS shows the outside edge turned up by as much as 3μm. This data could have been used for further polishing; however, the rms of their WEGU non-contact optical profilometer is 0.5μm, and convergence would be better with a more accurate measurement.

An attempt was made at JPL to use image-based measurements to quantify the edge error. The goal was sufficient accuracy to get the entire 85cm aperture within the range of an interferometer in one polishing cycle, without polishing too deep and creating a low spot. A simple optical system was used to illuminate the primary mirror (through the null lens) with narrowband visible white light and focus the returning beam onto a liquid nitrogen cooled CCD. Initially, phase retrieval and prescription retrieval methods were considered. Through-focus images can be used to accurately estimate the phase of the wavefront, and image matching in a raytrace/diffraction program can be used to estimate the errors on optical surfaces or in alignment. These methods have been used successfully on Hubble, Cassini, and other projects.[11,12] However, the images in this case were too noisy due to the large amount of light thrown around by the edge and by areas outside the intended clear aperture. Representative visible light images are shown in figure 6.

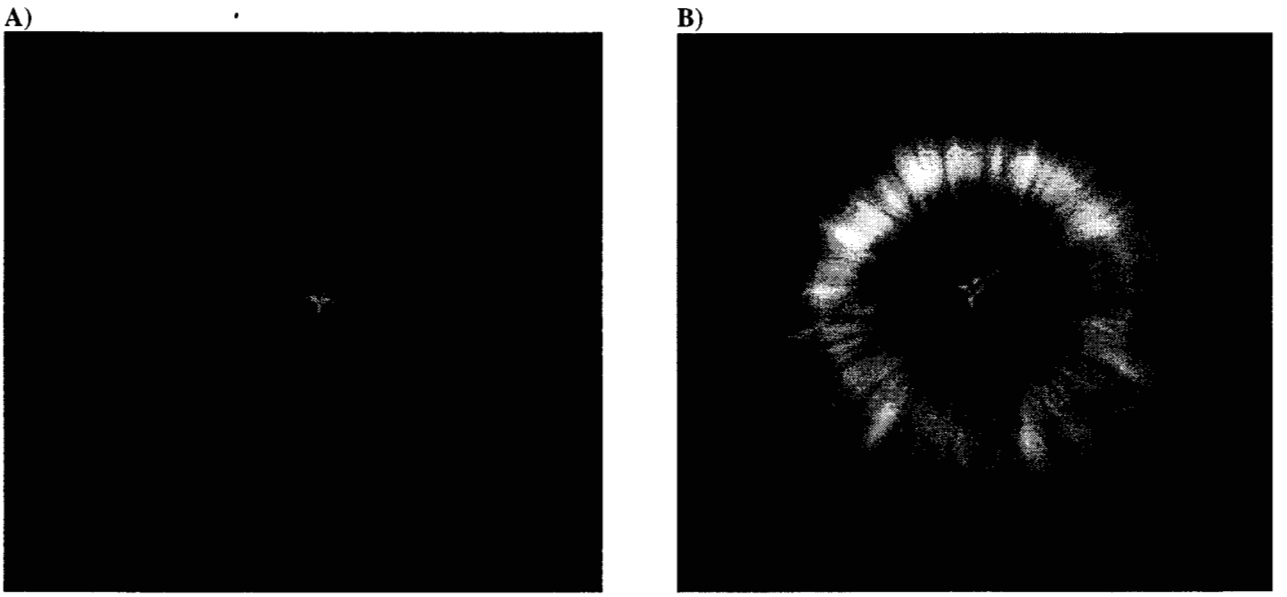

Figure 6. Visible light images: (A) nominally in-focus and (B) out-of-focus.

A physical optics model of this system would require 3.5μm pixels, much smaller than the 15μm pixels of the camera that was used, while maintaining its 16 bit dynamic range. To the best of our knowledge, such a camera does not exist. Furthermore, 4KX4K matrices would be needed for the calculations, too large for even the fast modern workstations at our disposal. Instead, a geometric analysis was conducted to estimate the edge. By changing focus, the contribution to the image from the edges can be separated from the rest of the image (figure 7).

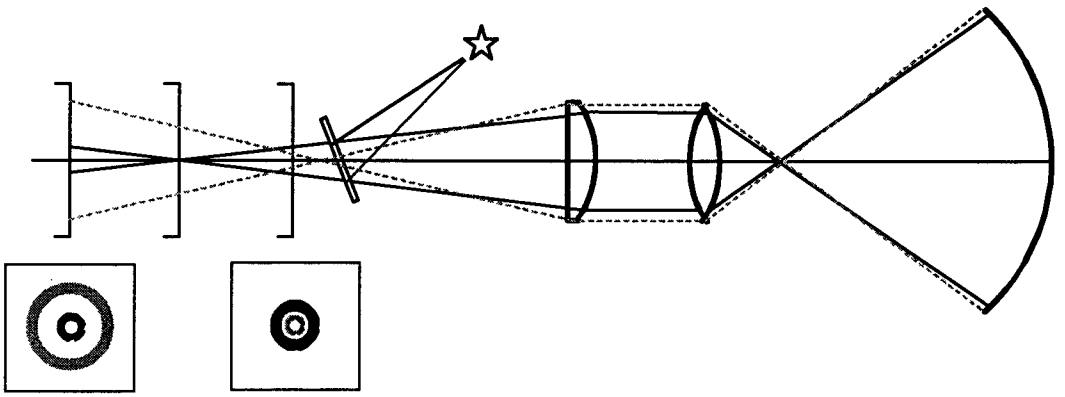

Figure 7. Images at different focus positions, including rays from the upturned edge.

Saturated images were taken to get sufficient signal strength in those areas of the image resulting from the steep edge. Each image was divided into 16 azimuthal sections. The edges were identified by graphically tracing the halo in the image; two sets of images with slightly different vignetting in the system were used to identify as much of the edge as possible (figure 8). Automated identification was not feasible due to streak-like structures in the image. (The source of these streaks is unknown; they could be from unpolished regions on the very outside or inside of the mirror.) The test setup was modeled in MACOS (Modeling and Analysis for Controlled Optical Systems), an in-house JPL raytrace and diffraction code. A deformable mirror surface type was used to simulate the primary mirror. The mirror surface was adjusted to match the observed intensity in a series of through-focus images, while maintaining a smooth variation of slope. The resulting edges were added to interferometric results to form a composite image. The accuracy of the result was estimated to be 25%, assuming no error in the boundary conditions. However, the amount of vignetting assumed for the analysis proved to be insufficient, and time pressures did not permit further study.

A)

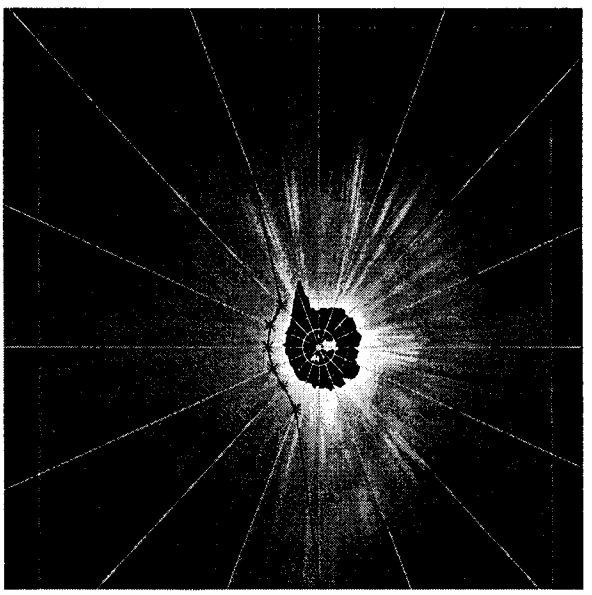

B)

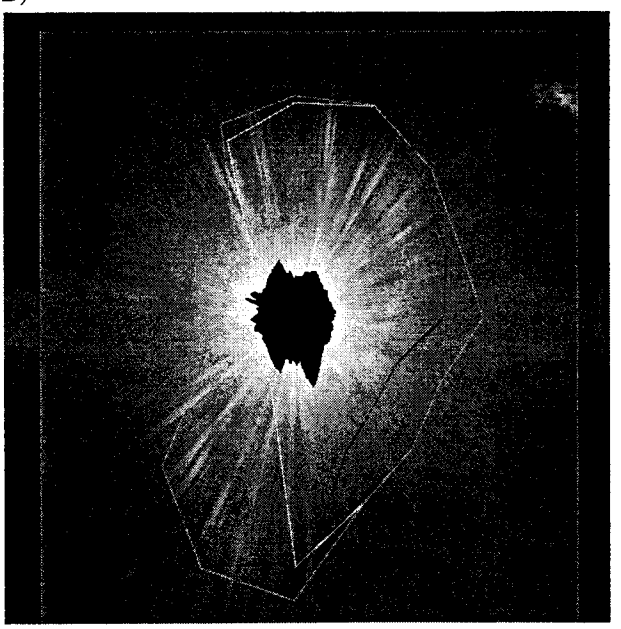

Figure 8. Saturated images, shows edge identification. (A) vignetting on left side of image; (B) vignetting on the right side, with left side results overlaid.

Boundary conditions were assumed based on the edge of the interferometric data and an 85cm mirror aperture. Neither assumption turned out to be valid. In the HDOS WEGU measurements, the edge turns up at a different place than the edge of the interferogram. The difference is about 1 cm in radial position; no good explanation has accounted for this. On the outside edge, there was no way to install a hard aperture stop at 85cm. A radial fiducial was created to determine the actual edge of the mirror as seen at the camera. The null lens focus was adjusted to trace out the steeper zones of the mirror. The limit was actually several cm short of the targeted 85cm due to vignetting in the setup.

Several sources of vignetting were identified. One is apertures inside the chamber for thermal control; these have since been expanded to reduce their contribution in the future. At times the cold shutter in the tank did not close completely and caused noticeable clipping on one side of the interferograms. Another source is vignetting inside the interferometer. A pinhole forms a field stop to clip rays returning at steep angles, to limit stray light entering the interferometer and eliminate rays with significant retrace error. However, images taken through a port on the interferometer, which bypasses the imaging optics and pinhole, still showed significant vignetting, so the contribution of the pinhole was relatively small. The pinhole had no contribution for the image-based tests since the interferometer was not in the optical system. A final vignetting source, which was not anticipated during the geometrical analysis, is the lens apertures inside the null lens. The null lens design used a perfect primary mirror with a clear aperture of 85cm to set the required apertures, with some margin to account for assembly errors. However, returning rays from an upturned edge, possibly even where the wavefront is not too steep for interferometric measurement, will pass through the null lens at a larger distance from the optical axis (see figure 7). This cannot be corrected without redesigning the null lens to make the lens apertures oversized or determine them by considering vignetting from an imperfect test mirror with a turned up edge.

Recent discussions have included characterizing the edge using a profilometer at Lick Observatory.

5. CONCLUSION

Test results for the ITTT beryllium primary mirror were presented. Cryo-null figuring resulted in an acceptable level of surface figure error (0.15λ rms) over an approximately 79cm aperture at low temperature, with one polishing cycle reducing the initial error by a factor of four. No thermal hysteresis was observed through many cryogenic cycles. Modeling of the residual error, assuming a corrected edge, predicts little impact of mid-spatial frequency errors on performance at wavelengths above 6.5μm and a strong influence on the PSF for visible wavelengths. Various measurements of the upturned edge were attempted, but none so far has given satisfactory accuracy. Future profilometry measurements may yet enable a single polishing cycle to take the entire 85cm clear aperture inside the capture range of an interferometer.

6. ACKNOWLEDGMENTS

This work, particularly the high-speed effort to conduct an image-based test, would not have been possible wthout the assistance of many people. In particular, Bob Debusk and Randy Hein provided immeasurable support in setting up the test. We also thank Dave Pearson, Jim Hardy, and Mark Lysek for scheduling around us while keeping the STTF running smoothly.

The optical metrology presented was conducted at the Jet Propulsion Laboratory, California Institute of Technology, under contract with the National Aeronautics and Space Administration. The optics were fabricated at Hughes Danbury Optical Systems.

7. REFERENCES

1. J. L. Fanson, D. J. Tenerelli, J. R. Houck, G. H. Rieke, G. G. Fazio, T. Kelly, and M. Whitten, "Space infrared telescope facility (SIRTF)," Proc. Soc. Photo-Opt. Instrum. Eng. **3356** (1998).
2. M. D. Bicay, M. W. Werner, and L. L. Simmons, "Space infrared telescope facility (SIRTF) enters development," Proc. Soc. Photo-Opt. Instrum. Eng. **3356** (1998).
3. D. R. Coulter, S. A. Macenka, M. T. Stier, and R. A. Paquin, "ITTT: a state-of-the-art ultra-lightweight all-Be telescope," Proc. Soc. Photo-Opt. Instrum. Eng. **CR67,** 277-296 (1997).

4. D. R. Coulter, S. A. Macenka, M. J. Lysek, and M. E. Larson, "The SIRTF telescope test facility," Proc. Soc. Photo-Opt. Instrum. Eng. **2744,** 745-750 (1996).
5. M. Larson, M. Lysek, D. R. Coulter, and S. A. Macenka, "The SIRTF telescope test facility: the first year," Proc. Soc. Photo-Opt. Instrum. Eng. **2814,** 2-7 (1996).
6. M. T. Stier, R. R. Crout, L. J. Cernoch, D. A. Hansen, M. H. Krim, A. L. Nonnenmacher, R. A. Paquin, G. P. Ruthven, F. R. Sileo, and J. Vollaro, "Telescope design for the infrared telescope technology testbed," Proc. Soc. Photo-Opt. Instrum. Eng. **3356** (1998).
7. G. C. Augason, J. A. Young, R. K. Melugin, D. S. Clarke, S. D. Howard, M. Scanlan, S. Wong, and K. C. Lawton, "Compensation for 6.5K cryogenic distortion of a fused quartz mirror by refiguring," Soc. Photo-Opt. Instrum. Eng. **1765** (1992).
8. CodeV® is a product of Optical Research Associates.
9. H. P. Stahl, D. Radacsi, T. J. Heydenburg, A. Gehan, R. P. Bourgeois, B. Radomski, D. A. Hansen, K. Kearney, M. T. Stier, S. A. Macenka, "Fabrication and testing of the ITTT beryllium secondary mirror," Proc. Soc. Photo-Opt. Instrum. Eng. **3134,** 62-71 (1997).
10. A. K. Mainzer, R. W. van Bezooijen, E. T. Young, T. H. Jamieson, A. E. Lowman, S. Sarfati, H. Mora, and N. Acu, "Pointing calibration and reference sensor for the space infrared telescope facility," Proc. Soc. Photo-Opt. Instrum. Eng. **3356** (1998).
11. D. Redding, P. Dumont, and J. Yu, "Hubble space telescope prescription retrieval," Appl. Opt. **32**, 1728-1736 (1993).
12. J. R. Feinup, J. C. Marron, T. J. Shulz, and J. H. Seldin, "Hubble space telescope characterized by using phase-retrieval algorithms," Appl. Opt. **32**, 1747-1767 (1993).